PAPER • OPEN ACCESS

Construction of realistic hybrid computational fetal phantoms from radiological images in three gestational ages for radiation dosimetry applications

View the article online for updates and enhancements.

Physics in Medicine & Biology

IPEM Institute of Physics and Engineering in Medicine

PAPER

Construction of realistic hybrid computational fetal phantoms from radiological images in three gestational ages for radiation dosimetry applications

Rasha Makkia[1], Keith Nelson[2], Habib Zaidi[3,4,5,6] and Michael Dingfelder[1]

[1] Department of Physics, East Carolina University, Greenville, NC, United States of America
[2] Department of Obstetrics and Gynecology, East Carolina University, Greenville, NC, United States of America
[3] Division of Nuclear Medicine and Molecular Imaging, Geneva University Hospital, CH-1211 Geneva, Switzerland
[4] Geneva Neuroscience Center, Geneva University, Geneva, Switzerland
[5] Department on Nuclear Medicine and Molecular Imaging, University of Groningen University Medical Center Groningen, Groningen, Netherlands
[6] Department of Nuclear Medicine, University of Southern Denmark, DK-500 Odense, Denmark

E-mail: makkiar13@gmail.com and dingfelderm@ecu.edu

Keywords: hybrid phantoms, fetus, segmentation, 3D modeling, NURBS, radiation dosimetry

Abstract

Radiation exposure and associated radiation risks are major concerns for fetal development for pregnant patients who undergo radiation therapy or diagnostic imaging procedures. In order to accurately estimate the radiation dose to the fetus and assess the uncertainty of fetal position and rotation, three hybrid computational fetus phantoms were constructed using magnetic resonance imaging (MRI) for each fetus model as a starting point to construct a complete anatomically accurate fetus, gravid uterus, and placenta. A total of 27 fetal organs were outlined from radiological images via the Velocity Treatment Planning System. The DICOM-Structure set was imported to Rhinoceros software for further reconstruction of 3D fetus phantom model sets. All fetal organ masses were compared with ICRP-89 reference data. Our fetal model series corresponds to 20, 31, and 35 weeks of pregnancy, thus covering the second and third trimester. Fetal positions and locations were carefully adapted to represent the real fetus locations inside the uterus for each trimester of pregnancy. The new series of hybrid computational fetus models together with pregnant female models can be used in evaluating fetal radiation doses in diagnostic imaging and radiotherapy procedures.

1. Introduction

Radiation exposure risks for the fetus are a major concern for pregnant patients who undergo radiation therapy or diagnostic imaging procedures (Martin 2011, Xie and Zaidi 2016). The number of patients undergoing radiation therapy has increased because of the noticeable improvement in cancer detection, treatment, and survival of patients. However, these patients are at higher risk for secondary malignancies due to their radiation exposure (Kry *et al* 2007). These concerns extend to the fetus if the mother is treated with radiation during pregnancy. The AAPM Radiation Therapy Committee Task Group 36 (TG-36) reported in 1995 that up to 4000 pregnant women receive radiotherapy treatment every year in the United States (Stovall *et al* 1995). Cancer is the number one cause of death in women aged 35 to 54 years. The most common invasive cancer types in pregnant women are breast cancer, cervical cancer, lymphoma, malignant melanoma, and thyroid cancer (Rimawi *et al* 2016, Zagouri *et al* 2016).

During many phases of the pregnancy, the fetus is highly sensitive to radiation, and irradiation during these times will increase fetus risks based on the dose-response relationship (Stovall, *et al* 1995). During the early stages of pregnancy, between gestational weeks 1–7, radiation exposure results in loss of normal cell developments, usually causing the loss of the fetus. If radiation exposure occurs between gestational weeks 8–25, the central nervous

system may be damaged, and the result can include potential fetal developmental delay or IQ reduction (Stovall *et al* 1995, Surbone *et al* 2008). Although it is impossible to avoid all radiation exposure to the fetus during radiation therapy procedures, shielding the unexposed abdominal region of the mother with a lead-rubber apron can significantly reduce the external radiation dose scatter. This is particularly important between gestational weeks 8–25, but such aprons are not always available (Stovall *et al* 1995). The radiation effects on the fetus are not well understood and cannot be predicted with certainty, but it is observed that the severity and frequency of adverse deterministic effects increase with total radiation dose and the probability of their occurrence is directly dependent on radiation dose.

Physical anatomical phantoms for radiological use were first introduced in the 1910s, and models for radiation dosimetry and radiation protection dosimetry in the late 1950s. (Lee and Lee 2006, Xu *et al* 2007). Because it is difficult to estimate the total radiation dose received by the human body that has been exposed to external and internal radiation, physicists developed computational phantoms to simulate the human body for dose measurements. Computational anthropomorphic phantoms are classified into three types: stylized phantoms, voxelized phantoms, and hybrid phantoms (Zaidi and Tsui 2009).

Stabin *et al* (1995) and Chen (2004) introduced the first mathematical stylized human fetus models set at the end of each trimester for nuclear medicine applications. With basic building shapes and simple surface equations, these models are considered very elementary and geometrically flexible. As a result of this simplification, the stylized model lacks appropriate information about organ locations and overall shapes to represent a realistic human body. Voxelized models have become promising only after sufficient advances in computational power and medical imaging technology from the 1980s to the 2000. These voxel-based models use computed tomography (CT) or magnetic resonance (MR) images of humans (Zaidi and Tsui 2009, Xie *et al* 2018a). A recent study reviewed the construction of voxel-based fetal phantoms of twins at 25 and 35 weeks of gestation who underwent positron emission tomography PET/CT scanning (Xie and Zaidi 2016, Xie *et al* 2018b). The voxelized fetal phantom set was entirely created from a few existing fetuses and newborn models which were scaled to the fetal gestational target. Even though the anatomical details of the voxelized phantom are improved from the stylized model, the fetal organ models were either adopted or scaled to a known parameter, e.g. average volume or mass, resulting in a loss of fidelity to the real patient structures. The resolution of the image slices used to develop those phantoms was limited to 7 mm thickness, causing an inevitable loss of the details of the fetal anatomy (Shi and Xu 2004). Becker *et al* segmented a 24 week of gestation fetus from an abdominal MR image of a patient and modified their already existing reference female voxel phantom Katja accordingly to create a virtual pregnant model for dose calculations (Becker *et al* 2008).

The third type of computational phantoms, referred to as hybrid phantoms, were first developed by Xu *et al* in the 2000s (Xu *et al* 2007). Hybrid phantoms incorporate organ boundaries and outer body contours described by combinations of polygon meshes. Obtaining whole body images of a pregnant patient is rarely medically necessary, nor practical or ethical due to the potential radiation exposure to the fetus, so hybrid phantoms were needed that took advantage of 3D surface modeling technologies to fill gaps in the voxel-based models. Xu's group released a set of hybrid pregnant phantom models with limited anatomical components derived from one CT image set of a pregnant patient at seven months of gestation. The fetus was scaled to match the International Commission of Radiological Protection (ICRP) standards of weight in order to represent three different gestational ages (Xu *et al* 2007). Maynard *et al* developed the University of Florida (UF) family of hybrid human fetus phantoms (Maynard *et al* 2014). While all major soft organs were modeled, a scaling technique was used to construct the other target gestational ages. A recent study developed three hybrid pregnant reference phantoms for nuclear medicine applications (Hoseinian-Azghadi *et al* 2014, Rafat-Motavalli *et al* 2016, Rafat-Motavalli *et al* 2018). The fetal models were generated from CT and MR images of five fetal specimens (8 - 28 weeks of gestation) and 2 sets of pelvic MR images from pregnant patients (22 and 38 weeks of gestation) to include 21 different organs.

To date, there is still a need for realistic hybrid computational fetal models developed from patient specific individual medical imaging sets for separate gestational ages to estimate radiation dose. Almost all other previously developed models were either scaled or adopted from one reference model or medical imaging set. As a result, the previous fetal models lack realistic anatomy, positioning, and posture of the fetus in utero.

This work is the first part of a larger project to study the effect of overweight and obesity on dose estimations for pregnant patients for imaging and therapy procedures. The focus of this manuscript is to develop a series of realistic computational fetal phantom model sets derived from pregnant patients at different gestational ages. They can then be used together with pregnant female phantoms to accurately estimate the radiation dose to fetal organs when a pregnant patient receives radiation therapy or diagnostic imaging procedures. The secondary goal of this work is to evaluate how this realistic hybrid phantom compares to the ICRP standard fetal model (ICRP 2002).
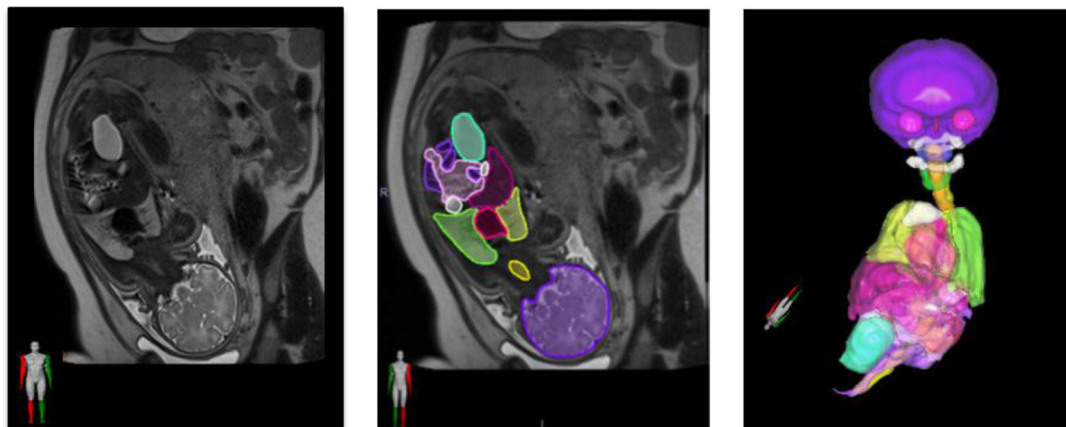
Figure 1. Sagittal MR images of a pregnant patient at 35 weeks of gestation, demonstrating segmentation using the Velocity TPS and the delineated 3D model exported in DICOM-Structure format.

2. Materials and methods

2.1. Target fetal ages

A total of three fetal ages: 20, 31, and 35 weeks of gestation were chosen to represent fetal organ anatomical development for the second and third trimesters. Because the pregnant patient does not typically undergo x-ray or CT imaging in the first trimester, very limited image sets were available for early pregnancy. In the one first-trimester study available (12 weeks of gestation), maternal organs were not well defined, so the image set was excluded from this study. Our target models, therefore, represent the middle second and third trimesters. A total of nine MR sets were used for this study to develop fetal computational phantoms.

2.2. Image acquisition

Three computational phantoms were constructed, starting from de-identified high-quality MR images to build a complete anatomically accurate fetus, gravid uterus, and placenta. All radiological images in DICOM format were anonymized under an approved Institutional Review Board (IRB) protocol from Vidant Medical Center in Greenville, North Carolina. All images were screened by an obstetrician-gynecologist to confirm normal anatomy and complete coverage of the fetus before segmentation. The MR images were acquired in a 1.5 T static field strength performed on a Signa HDxt (GE Healthcare). Independent sagittal, axial, and coronal T2-weighted scans were performed using typical acquisition parameters including flip angle $= 90°$, Field-of-view (FOV) $= 480$, slice thickness/gap $= 2/1.3$ mm, matrix $= 512 \times 512$ pixels, and voxel sizes $(2\,\text{mm})^3$.
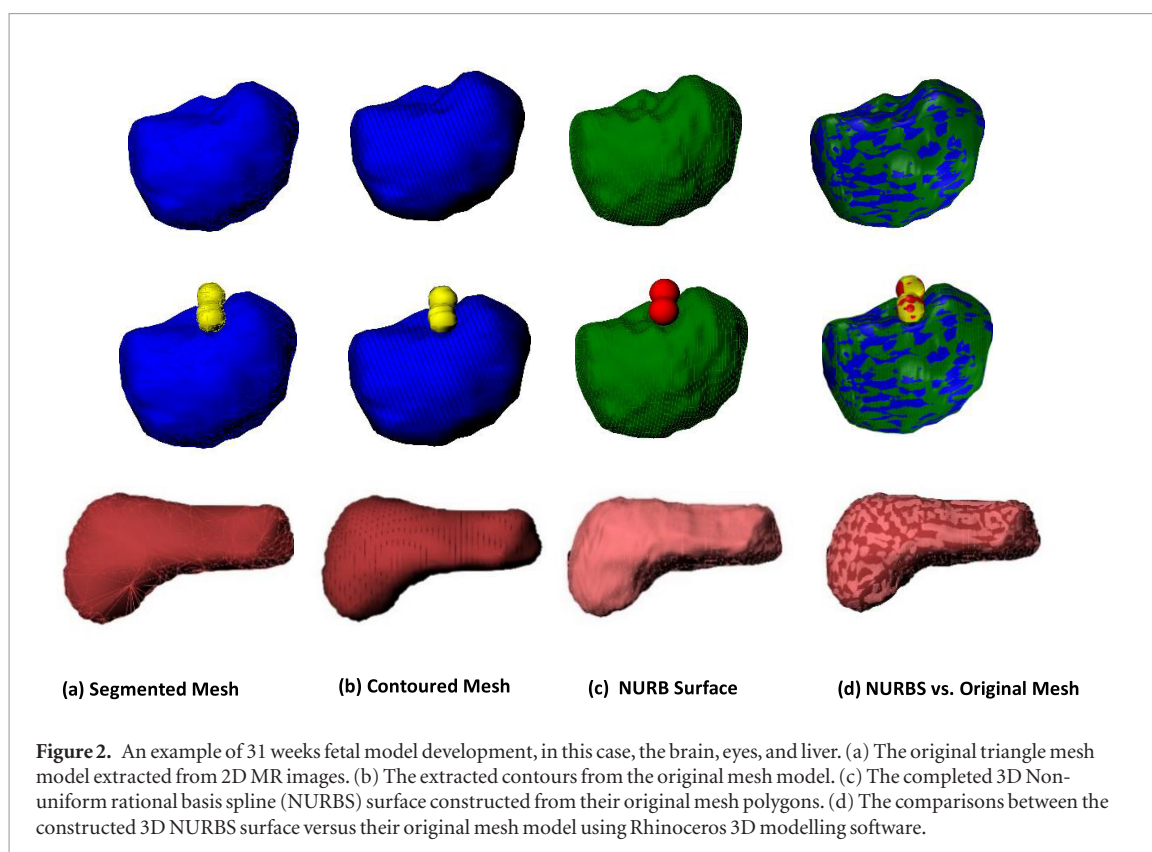
2.3. Image segmentation

Image segmentation was performed to isolate and define several individual organs and structures. The segmentation of MR image sets was performed on a clinical contouring tool using the Velocity 3.1 Treatment Planning System (TPS) (Varian Medical Systems, Palo Alto, CA). The original MR images including the sagittal, axial, and coronal views in DICOM format were directly imported into the Velocity TPS. The anatomical structures of interest were contoured slice by slice and segmented manually; no automatic segmentation was applied to any of the images. The process of contour extraction and 3D surface developing are illustrated in figure 1. The following structures were identified: uterus, placenta, umbilical cord, fetal body, amniotic fluid, brain, eyes, tooth buds, pituitary gland, thymus, thyroid, tongue, trachea, bronchus, lungs, liver, heart, esophagus, stomach, small intestine, large intestine, kidneys, adrenal glands, pancreas, spleen, spine, spinal cord, urinary bladder, and gallbladder. As for bone structures, only the spine was segmented from MR images for each gestation period. Because the thyroid and adrenal glands could not be confidently identified in the 20-week image sets, models were created and added based on their suitable locations (Isaacson *et al* 1986, Nelson *et al* 1988). All organ segmentations, locations, and overall shapes were verified and approved by one of the authors (KN).

2.4. NURBS and polygon mesh modeling

Once all of the fetal structures were identified and segmented, the DICOM-Structure set was exported from Velocity TPS. 3D Slicer 4.6 (Kikinis *et al* 2014) was used to generate a 3D polygon mesh in a format called a Wavefront Object (OBJ). The polygon mesh was then imported into Rhinoceros™ 6.0 (Rhinoceros, McNeel North America, Seattle, WA). Rhinoceros software offers many tools for 3D geometry manipulation, such as deformation, fitting, scaling, volume checking, editing, and surface rendering. These tools were used to create a

Table 1. Computed fetal organ masses and densities at three gestational ages compared with ICRP-89 reference data (ICRP 2002).

Tissue	Density (g cm⁻³)	This work volume (cm³)			This work mass (g)			ICRP-89 reference mass (g)			Percentage error		
		20 w	31 w	35 w	20 w	31 w	35 w	20 w	31 w	35 w	20 w	31 w	35 w
Adrenal glands	1.03	0.95	3.08	4.41	0.98	3.10	4.54	0.98	3.00	4.60	0.17	3.33	1.23
Amniotic fluid	1.00	542.60	4236.88	3554.54	542.60	4236.88	2186.15	350.00	750.00	725.00	55.03	464.92	201.54
Brain	1.03	72.31	339.38	343.00	74.48	349.56	353.29	62.00	213.57	300.00	20.13	63.67	17.76
Bronchi	1.07	0.04	0.13	0.34	0.04	0.14	0.37	—	—	—	—	—	—
Eyes	1.03	1.87	6.28	9.60	1.93	6.47	9.89	—	—	—	—	—	—
Eye lenses	1.07	0.40	0.90	1.02	0.43	0.96	1.09	—	—	—	—	—	—
Fetal body	1.03	355.13	1767.00	2443.00	365.78	1820.01	2516.29	300.00	1500.00	2800.00	21.93	21.33	10.13
Gallbladder	1.03	0.62	1.02	1.23	0.64	1.05	1.27	—	—	—	—	—	—
Heart	1.04	4.45	21.92	29.50	4.63	22.80	30.68	3.00	10.57	15.00	54.27	115.64	104.53
Intestines	1.03	16.60	71.00	68.00	17.10	73.13	70.04	—	—	—	—	—	—
Kidneys	1.03	2.85	26.10	21.70	2.94	26.88	22.35	3.80	13.88	20.00	22.75	93.65	11.76
Liver	1.04	13.76	94.60	122.42	14.31	98.38	127.32	19.00	67.28	100.00	24.69	46.23	27.32
Lungs	1.04	21.84	62.41	107.10	22.71	64.91	111.38	15.00	40.58	51.00	51.42	59.95	118.40
Nasal septum	1.03	0.23	0.77	0.29	0.24	0.79	0.30	—	—	—	—	—	—
Pancreas	1.03	2.24	3.92	4.39	2.31	4.03	4.53	2.30	4.06	4.50	0.31	0.63	0.57
Pituitary gland	1.03	0.05	0.07	0.08	0.05	0.07	0.08	—	—	—	—	—	—
Spinal cord	1.02	2.33	1.71	1.81	2.38	1.74	1.86	—	—	—	—	—	—
Spine	1.03	8.04	12.20	19.61	8.28	12.57	20.20	—	—	—	—	—	—
Spleen	1.04	0.34	1.07	3.01	0.36	1.11	3.13	0.36	2.88	5.80	1.29	61.33	45.97
Stomach	1.00	3.78	6.03	12.20	3.78	6.03	12.20	—	—	—	—	—	—
Tongue	1.05	0.75	3.40	4.28	0.79	3.57	4.49	—	—	—	—	—	—
Tooth buds	1.22	0.79	4.09	6.13	0.97	4.99	7.48	—	—	—	—	—	—
Trachea	1.07	0.77	2.07	5.64	0.82	2.22	6.03	—	—	—	—	—	—
Thymus	1.07	1.36	4.20	3.28	1.46	4.49	3.51	1.50	6.19	9.70	2.99	27.44	63.82
Thyroid gland	1.05	0.17	0.60	0.95	0.18	0.63	1.00	0.18	0.67	1.00	0.62	6.36	0.25
Umbilical cord	1.04	21.33	73.60	127.00	22.18	76.54	132.08	—	—	—	—	—	—
Urinary bladder	1.01	1.52	8.29	19.90	1.54	8.37	20.10	—	—	—	—	—	—
Maternal placenta	1.04	98.58	1361.00	550.90	102.52	1415.44	572.94	170.00	459.18	565.00	39.69	208.25	1.40
Maternal uterus	1.03	1003.00	7329.00	5148.00	1033.09	7548.87	5407.46	430.00	683.30	950.00	140.25	1004.77	469.21

Figure 2. An example of 31 weeks fetal model development, in this case, the brain, eyes, and liver. (a) The original triangle mesh model extracted from 2D MR images. (b) The extracted contours from the original mesh model. (c) The completed 3D Non-uniform rational basis spline (NURBS) surface constructed from their original mesh polygons. (d) The comparisons between the constructed 3D NURBS surface versus their original mesh model using Rhinoceros 3D modelling software.

non-uniform rational basis spline (NURBS) surface for each structure as illustrated in Xu and Eckerman (2010). The contour and loft commands were used to create a spaced series of planar curves around the outer shape of a given polygon mesh organ along a user-defined axis. The loft command was also used to fit a surface through created profile curves that defined the surface shape from the contours command, wrapping NURBS surfaces around the specified volume. The original polygon meshes were no longer needed after creating NURBS surfaces for many organs. Figure 2 shows an example of using the contour and loft tools to form a 3D NURBS surface representation of the brain, eyes and liver of the 31-week fetus. The following organs were modeled with NURBS surfaces: brain, heart, kidneys, liver, lungs, pancreas, spleen, stomach, thymus, trachea, gallbladder, urinary bladder, pituitary gland, thyroid gland, uterus, and placenta. The fetal body, spine, spinal cord, umbilical cord, tongue, tooth buds, small and large intestines were kept as a polygon mesh due to their complexity or difficulty in approximating them as a NURBS surface. Eyes and lenses were replaced with spherical and ellipsoid objects that matched the initially segmented organs.

3. Results

3.1. Comparing fetal organ masses with ICRP reference values

The complete organ masses and densities of the 20, 31, and 35 weeks fetal phantoms, as well as the ICRP-89 reference masses (ICRU 1992, ICRP 2002) are presented in table 1. Since the computational phantoms are volume-based, mass densities were required to convert between organ volumes and organ masses. Masses reported in table 1 were obtained from Rhinoceros™ with much effort taken to keep NURBS surfaces or mesh polygon volumes matched with the same original organ volumes that were obtained from the DICOM-structure file when converting to NURBS surfaces for each fetus model. In addition, the fetal soft tissue densities and fetal organ masses were adopted from ICRP-89 (ICRP 2002) and ICRU Report 46 (ICRU 1992). The percentage differences between the derived/calculated fetal organ masses and the average values reported in ICRP-89 is also shown in table 1. While total fetal masses are within 10%–20% of the average ICRP-89 reference values, individual organs differ up to a factor 2 in size/mass, for example the heart and lungs. All three mothers were heavy-weight, with the mother with the 31 week fetus obese. This is reflected in the partially large and strong varying values for amniotic fluids, placenta, and maternal uterus.

    Fetus size and mass were independently estimated in regular prenatal examinations using ultrasound (US) imaging. They are based on measured and visible volumes in these US data and are a rough estimate. US data for the 20 week fetus obtained nine days before the MR images were acquired indicated that the fetus was at the 60th percentile of overall growth with a total mass of 353 g. US data of the 31 week fetus data recorded two days
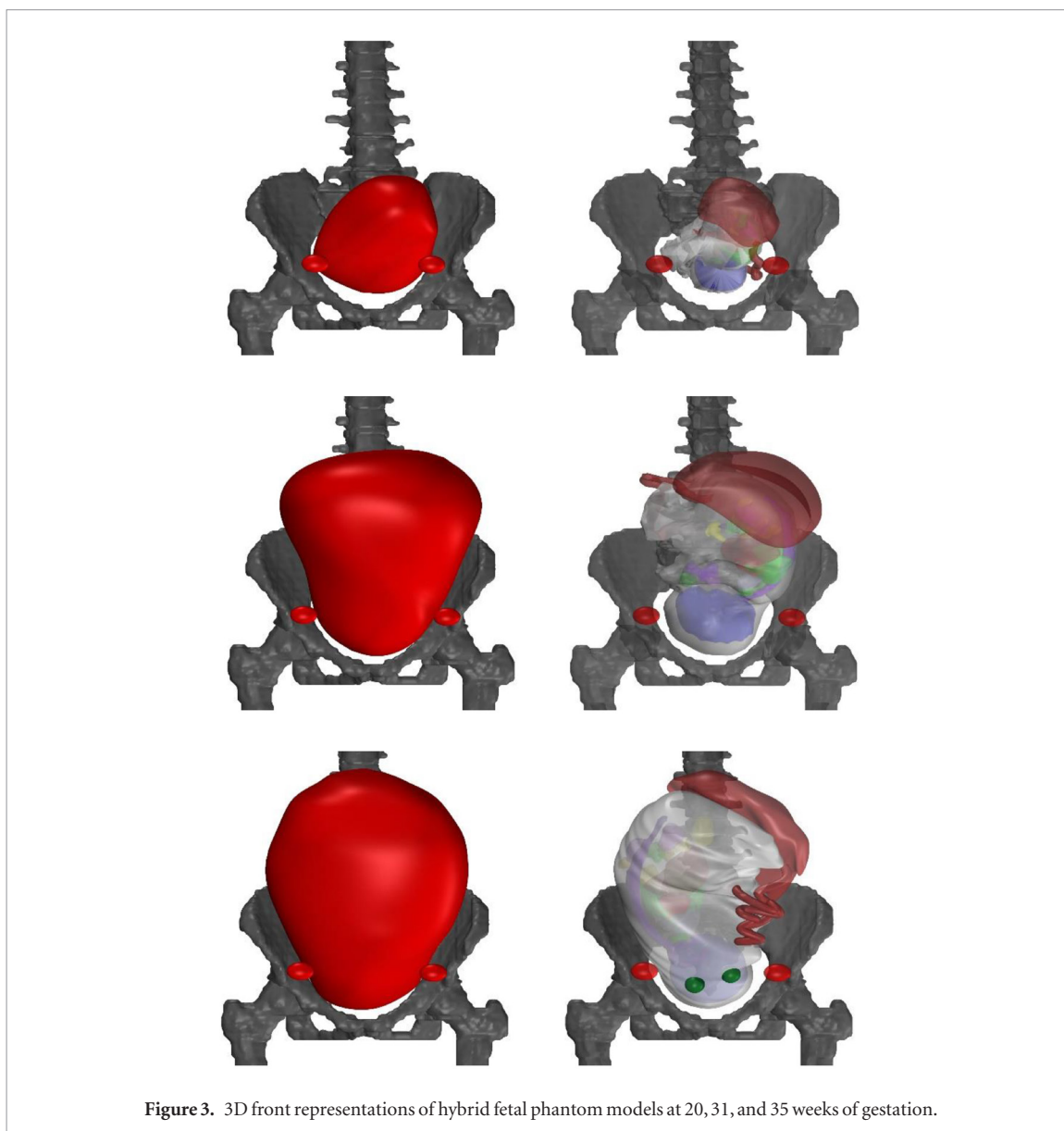
Figure 3. 3D front representations of hybrid fetal phantom models at 20, 31, and 35 weeks of gestation.

after MR images were taken also indicated that the fetus was larger than average with a total mass of 2223 g, or at the 75 percentile of growth overall. While the 20 and 31 week fetuses were larger than average, US data of the 35 week fetus obtained nine days after the MR images were acquired indicated a total fetus mass of 2630 g which corresponds to the 45th percentile of overall growth. US acquired fetus masses agree well with the calculated values from the MR images and explain the observed variation in the data mass compared to the average ICRP-89 values, as reported in table 1.

3.2. Fetus position in utero

The fetal positioning or orientation has not been clearly specified in the radiation dosimetry literature. The fetus is actively mobile throughout the pregnancy with a gradually increasing probability of being encountered in the head-down position as the pregnancy progresses to term. All fetus locations were carefully adjusted to reflect the original fetus position inside the maternal uterus for a realistic and consistent modeling. All fetus models were head down with the 20 weeks of gestation model in the right occiput posterior (ROP) configuration, the 31 weeks of gestation model in the left occiput anterior (LOA) configuration, and the 35 weeks of gestation model again in the ROP configuration, all surrounded by the maternal tissues including the placenta and uterus. A 3D front representation of all three models in head down position is presented in figure 3.

4. Discussion

In this work, three independent hybrid fetus phantom models were constructed from individual patient-specific MR images. The three models represent 20, 31, and 35 weeks of gestation and are obtained from different

patients. Each fetal model contains 27 different organs and tissues segmented from the MR images and modeled with NURBS and polygon meshes. This allows in keeping very small structures for a realistic anatomy and not compromising resolution when voxelizing models. Each fetal model is based on an individual patient-specific data set. Together, they represent a wide variety of realistic fetal anatomy which is changing with gestation. These fetal models are not scaled from each other or normalized to ICRP average values, as it is standard in the majority of other models in the literature to represent gestation age. These hybrid fetus models have many advantages that make them suitable for various applications since they offer the flexibility to maintain the original mesh shapes and the anatomic accuracy by using real medical image sets for each model. Fetus position and orientation can be adjusted easily as shown in the front view head down orientations for all three models in figure 3.

All three fetal phantom models are based on patient-specific MR images and illustrate a wide variety of organ sizes and exact positions, away from the standardized mean. The existing ICRP-89 reference phantoms represent the population average and are designed for prospective radiation protection studies with normalized data to provide recommendations for the general public. However, diagnostic imaging or radiation treatment planing requires patient-specific data for accurate dosimetry and risk assessment. Especially the heavy weight and obese cases will help to better understand limitations and uncertainties associated with these tasks when these fetal models are combined with standard, heavy weight or obese pregnant female phantom models available in the literature.

The fetus phantoms in this work including the NURBS and polygon meshes can be used for future evaluations of the radiation dose and radiation risk to the fetus and fetus organs in radiation protection, medical imaging, and radiation therapy in conjunction with Monte Carlo radiation transport simulations. Hybrid phantoms, including the hybrid fetus phantoms, are used to provide average and extreme geometries for radiation transport calculations. This will allow for better estimate mean doses including uncertainties, and more realistic risks.

5. Conclusion

These newly developed hybrid fetal computational models at 20, 31, and 35 weeks of gestation, based on real imaging sets of pregnant patients, were composed of NURBS and polygon mesh surfaces which are powerful mathematical tools for phantom construction. NURBS-based fetal hybrid phantoms represent realistic human fetal anatomy and fetal position inside the uterus. The hybrid fetal computational models accurately reflect the existing computational standards from the ICRP and can be useful in evaluating radiation doses to the fetus and estimating risks to the pregnant patient seeking radiotherapy or diagnostic imaging where realistic fetal computational human-based phantoms are required. These newly developed fetus models can also be used for radiation protection purposes to expand its current definition of fetal references of a given population concerning the body weight.

Acknowledgments

ORCID iDs

Habib Zaidi ⓘ https://orcid.org/0000-0001-7559-5297
Michael Dingfelder ⓘ https://orcid.org/0000-0002-3171-3498

References

Becker J, Zankl M, Fill U and Hoeschen C 2008 Katja—the 24th week of virtual pregnancy for dosimetric calculations *Pol. J. Med. Phys Eng.* **14** 13–19

Chen J 2004 Mathematical models of the embryo and fetus for use in radiological protection *Health Phys.* **86** 285–95

Hoseinian-Azghadi E, Rafat-Motavalli L and Miri-Hakimabad H 2014 Development of a 9-months pregnant hybrid phantom and its internal dosimetry for thyroid agents *J. Radiat. Res.* **55** 730–47

ICRP 2002 *Basic Anatomical and Physiological Data for Use in Radiological Protection: Reference Values* (*ICRP Publication* 89, *Annal ICRP* vol 32) (Oxford: Pergamon)

ICRU 1992 *Photon, Electron, Proton and Neutron Interaction Data for Body Tissues* (*ICRU Report* vol 46) (Bethesda, MD: ICRU) p 24

Isaacson G, Mintz M C and Crelin E S 1986 *Atlas of Fetal Sectional Anatomy: With Ultrasound and Magnetic Resonance Imaging* (New York: Springer)

Kikinis R, Pieper S D and Vosburgh K G 2014 *3D Slicer Intraoperative Imaging and Image-Guided Therapy* (New York: Springer)

Kry S F, Followill D, White R A, Stovall M, Kuban D A and Salehpour M 2007 Uncertainty of calculated risk estimates for secondary malignancies after radiotherapy *Int. J. Radiat. Oncol.* **68** 1265–71

Lee C and Lee J 2006 Computational anthropomorphic phantoms for radiation protection dosimetry: evolution and prospects *Nucl. Eng. Technol.* **38** 239–50

Martin D D 2011 Review of radiation therapy in the pregnant cancer patient *Clin. Obstet. Gynecol.* **54** 591–601

Maynard M R, Long N S, Moawad N S, Shifrin R Y, Geyer A M, Fong G and Bolch W E 2014 The UF family of hybrid phantoms of the pregnant female for computational radiation dosimetry *Phys. Med. Biol.* **59** 4325–43

Nelson L H, Bo W J and Lynch G C 1988 *Fetal Sectional Anatomy and Ultrasonography* (Baltimore, MD: Williams & Wilkins)

Rafat-Motavalli L, Miri-Hakimabad H and Hoseinian-Azghadi E 2016 Fetal and maternal dose assessment for diagnostic scans during pregnancy *Phys. Med. Biol.* **61** 3596–608

Rafat-Motavalli L, Miri-Hakimabad H and Hoseinian-Azghadi E 2018 Hybrid pregnant reference phantom series based on adult female ICRP reference phantom *Radiat. Phys. Chem.* **144** 386–95

Rimawi B, Green V and Lindsay M 2016 Fetal implications of diagnostic radiation exposure during pregnancy: recommendations *Clin. Obstet.* **59** 412–8

Shi C and Xu X G 2004 Development of a 30-week-pregnant female tomographic model from computed tomography (CT) images for Monte Carlo organ dose calculations *Med. Phys.* **31** 2491–7

Stabin M G, Watson E E, Cristy M, Ryman J C, Eckerman K F, Davis J L, Marshall D and Gehlen M K 1995 *Mathematical Models and Specific Absorbed Fractions of Photon Energy in the Nonpregnant Adult Female and at the End of Each Trimester of Pregnancy* (Tennessee: Oak Ridge National Laboratory)

Stovall M, Blackwell C R, Cundiff J, Novack D H, Palta J R, Wagner L K, Webster E W and Shalek R J 1995 Fetal dose from radiotherapy with photon beams: report of AAPM Radiation Therapy Committee Task Group No. 36. *Med. Phys.* **22** 63–82

Surbone A, Peccatori F and Pavlidis N (ed) 2008 *Cancer and Pregnancy* (Berlin: Springer)

Xie T and Zaidi H 2016 Development of computational pregnant female and fetus models and assessment of radiation dose from positron-emitting tracers *Eur. J. Nucl. Med. Mol. Imaging* **43** 2290–300

Xie T, Poletti P-A, Platon A, Becker C D and Zaidi H 2018a Assessment of CT dose to the fetus and pregnant female patient using patient-specific computational models *Eur. Radiol.* **28** 1054–65

Xie T, Zanotti-Fregonara P, Edet-Sanson A and Zaidi H 2018b Patient-specific computational model and dosimetry calculations for PET/CT of a patient pregnant with twins *J. Nucl. Med.* **59** 1451–8

Xu X G and Eckerman K F 2010 *Handbook of Anatomical Models for Radiation Dosimetry* vol 30 (Boca Raton, FL: CRC Press)

Xu X G, Taranenko V, Zhang J and Shi C 2007 A boundary-representation method for designing whole-body radiation dosimetry models: pregnant females at the ends of three gestational periods—RPI-P3, -P6 and -P9. *Phys. Med. Biol.* **52** 7023–44

Zagouri F, Dimitrakakis C, Marinopoulos S, Tsigginou A and Dimopoulos M-A 2016 Cancer in pregnancy: disentangling treatment modalities *ESMO Open* **1** e000016

Zaidi H and Tsui B M W 2009 Review of computational anthropomorphic anatomical and physiological models *Proc. IEEE* **97** 1938–53